Research Article
doi.org/10.1002/slct.202301653
Chemistry Europe
European Chemical Societies Publishing
www.chemistryselect.org

exo-endo Isomerism of Carboranes: Unusual Geometries of $C_2B_5X_7$ (X = Cl, Br) and $C_2B_7Cl_9$ with *exo*-Skeletal BCl_2 Groups on Carbon Revealed by Joint Spectroscopic/Computational Studies

Willi Keller,*[a] Jürgen Conrad,[a] and Matthias Hofmann[b]

Reexamination of the co-pyrolysis reactions of B_2Cl_4 with C_2Cl_4 at 350 °C and of B_2Br_4 with CBr_4 at 300 °C *in vacuo* confirmed the carboranes $C_2B_5Cl_7$ (**1**), $C_2B_7Cl_9$ (**2**), and $C_2B_5Br_7$ (**3**) as low-yield products. While **1** only could be concentrated by repeated vacuum fractionation, **2** and **3** could now be isolated from the conglomerate mixtures for a full spectroscopic characterization and the compounds were verified in their geometries by detailed DFT computations. Surprisingly, the perhalogenated carboranes do not adopt the expected "all-*endo*"-geometries with cluster sizes derived by the sum of the n boron and two carbon atoms ($n+2$) as known from the syntheses of the parent *closo*-carboranes $C_2B_nH_{n+2}$. Instead, DFT/GIAO(ZORA)/NMR (GIAO for X = Cl, ZORA for X = Br) computations revealed that the perhalogenated carboranes favor structures with BX_2 groups as *exo*-skeletal ligands attached to both cage-carbon atoms yielding the five-vertex *closo*-1,5-$(CBX_2)_2B_3X_3$ (**1**: X = Cl; **3**: X = Br) and the seven-vertex *closo*-2,4-$(CBCl_2)_2B_5Cl_5$ for **2**. In contrast to these perhalogenated carboranes, analogous computations on the hydrogen substituted carboranes $C_2B_nH_{n+2}$, silaboranes $Si_2B_nH_{n+2}$ and $Si_2B_nX_{n+2}$ (n = 5, 7) show in all cases a thermodynamic favorization of structures where all boron atoms of the formula are *endo*-skeletally incorporated into the cluster frameworks.

Introduction

The starting point of the fascinating chemistry of the carboranes was set in 1962 by the pioneering report on the low-yield preparation of three compounds with the compositions $C_2B_3H_5$, $C_2B_4H_6$ and $C_2B_5H_7$ in a silent electric discharge reaction of pentaborane(9) with acetylene.[1] Although classical structures with localized *2c–2e* bonds could be suggested,[2] evaluation of spectroscopic data, structural analyses, electron density distribution, and ab initio calculations later proved closed deltahedral geometries with multicenter bonds for these compounds.[3] Until today, they represent the smallest experimentally proven members within the neutral *closo*-carborane family $C_2B_nH_{n+2}$, since a hypothetically smaller tetrahedral *closo*-$C_2B_2R_4$ is unknown which is rather found in a butterfly-type structure.[4] In search of alternative routes to carboranes from small precursory molecules, we studied the vacuum pyrolysis of suitable alkyldichloro-boranes and obtained hexachloro-hexabora-adamantane $C_4H_4B_6Cl_6$.[5] In this molecule, we could not replace the carbon bound H atoms by Cl ligands to study the effect of electron-withdrawing substituents on the molecular cohesion. One might expect the transformation to non-classical structures by a decrease of electron density. In a preliminary communication in 1989,[6] we reported on the preparation of mixtures of carboranes with the molecular formula $C_2B_5X_7$ (**1**: X = Cl, **3**: X = Br) and $C_2B_7Cl_9$ (**2**) by co-pyrolyzing B_2X_4 with halogenated hydrocarbons *in vacuo* at temperatures around 300 °C. On the basis of mass spectral and one-dimensional ^{11}B NMR data and our empirical experience with other heteroboranes prepared correspondingly, such as e.g. the phosphaborane *closo*-1,2-$P_2B_4Cl_4$,[7] where each boron and heteroatom of the respective formula was *endo*-skeletally incorporated into the cluster frameworks, we assumed "all-*endo*" *closo*-structures with geometries as derived by Wade's rules[8] for the respective parent carboranes $C_2B_nH_{n+2}$. However, these assignments were suggestive due to the lack of sufficient spectroscopic data. In particular, ^{11}B NMR chemical shifts – one for each carborane – in the low field between 50 and 60 ppm found in the ^{11}B NMR spectra of carboranes **1**–**3** were actually too low fielded for *endo*-polyhedral boron atoms of carboranes and rather support a classical *2c–2e* bonding situation for these boron atoms. These ambiguities prompted our extensive reinvestigations of the co-pyrolysis reactions of B_2X_4 with halogenated hydrocarbons to obtain more evaluable data for structural elucidation.

[a] *Dr. W. Keller, Dr. J. Conrad*
Institut für Chemie, Universität Hohenheim, Garbenstrasse 30, D-70599 Stuttgart, Germany
E-mail: willi.keller@uni-hohenheim.de
[b] *Dr. M. Hofmann*
Anorganisch-Chemisches Institut, Ruprecht-Karls-Universität Heidelberg, Im Neuenheimer Feld 270, D-69120 Heidelberg, Germany

Supporting information for this article is available on the WWW under https://doi.org/10.1002/slct.202301653

Results and Discussion

Generation of the reactive species

The thermal disproportionation of diboron tetrahalides B_2X_4 to the boron(I)- and B(III)-halides (Equation 1) starts already at −20 °C and completes at temperatures above 300 °C to the most stable boronsubhalide B_9X_9.[9] There is photolytic,[9] ESR[9] and PE[10] spectroscopic evidence that the reaction rather proceeds via [:BX] intermediates which aggregate to B_nX_n (for X = Cl: n = 8–12, Equation 2)[9] than via homolytic cleavage into two [·BX_2] units. As potential carbon sources for a co-pyrolysis, perhalogenated aliphatic compounds are known to thermally dehalogenate into various short-lived molecules and radical species (Equation 3) which can recombine to larger binary molecules as e.g. tetrahaloethene (Equation 4) or hexahalobenzene (Equation 5).[11] In accordance with the lower bond dissociation energy of C–Br compared to C–Cl, brominated hydrocarbons dehalogenate easier than chlorinated analogues. Suitable halogenated aliphates supply reactive carbon species at temperatures as low as possible without the abstraction of hydrogenhalides HX which could decompose potential haloborane products. Elemental halogen evolving in these decomposition processes can be trapped by B_2X_4 moieties (Equation 6), thereby providing a series of different molecules and molecular fragments for reactions and recombinations to binary (Equations 2, 4 and 5) or ternary (Equations 7–9) products:

$$B_2X_4 \rightarrow BX_3 + [BX] \quad (1)$$

$$n\ [BX] \rightarrow B_nX_n \quad (2)$$

$$CX_4 \rightarrow [CX_3]/[CX_2]/[CX] + X_2 \quad (3)$$

$$2\ [CX_2] \rightarrow C_2X_4 \quad (4)$$

$$6\ [CX] \rightarrow C_6X_6 \quad (5)$$

$$X_2 + B_2X_4 \rightarrow 2\ BX_3 \quad (6)$$

$$n\ [BX] + 2\ [CX] \rightarrow C_2B_nX_{n+2} \quad (7)$$

$$6\ B_2Cl_4 + C_2Cl_4 \rightarrow C_2B_5Cl_7 + 7\ BCl_3 \quad (8)$$

$$8\ B_2Cl_4 + C_2Cl_4 \rightarrow C_2B_7Cl_9 + 9\ BCl_3 \quad (9)$$

Studied co-pyrolysis reactions

The co-pyrolysis reactions of B_2X_4 with halogenated hydrocarbons confirmed our initially reported results. Pyrolyses were performed *in vacuo* with mixtures of a) B_2Cl_4/CCl_4 at 420 °C and 340 °C, b) B_2Cl_4/C_2Cl_4 at 300 °C to 350 °C, and c) $B_2Cl_4/CH(BCl_2)_3$ at 450 °C, the product mixtures were separated into more and less volatile fractions, and their NMR and MS spectra were recorded. Similarly, we investigated the reactions d) B_2Br_4/CBr_4 at 300 °C and e) B_2Br_4/C_2Br_4 at 220 °C. In experiments a), only the binary compounds C_6Cl_6, B_9Cl_9 and $B_{10}Cl_{10}$ could be detected in addition to volatile molecules such as BCl_3 or Cl_2. In order to get some insight into the mode of reaction, it seemed reasonable, to subject the reactants to milder conditions. When tetrachloroethene is used (experiment b), lower temperatures are sufficient for conversion. In this case, mass spectrometry reveals compounds with the *closo*-carborane compositions $C_2B_5Cl_7$ (**1**) and $C_2B_7Cl_9$ (**2**) in the more volatile fraction, and B_9Cl_9 and $B_{10}Cl_{10}$ in the less volatile fraction. The conversion mentioned in experiment c) leads to the bora-adamantane $C_4H_4B_6Cl_6$. During the co-pyrolysis with brominated synthons at 300 °C (experiment d), the carborane $C_2B_5Br_7$ (**3**) is formed, while under milder conditions at 220 °C (experiment e) tribromovinyl-dibromoborane, $Br_2C{=}CBr{-}BBr_2$ (**4**) is formed in addition to **3** and B_nBr_n (n = 7–10). The formation of **4** can be understood as the product of either the addition of B_2Br_4 to tetrabromoethene with subsequent BBr_3 elimination or as the insertion of the most readily formed [BBr] species into a C–Br bond. This molecule could function as an intermediate in the formation of the brominated carborane products, as depicted in Scheme 1, variation b).

The series of mass spectra are very typical due to the isotopic combinations and the low fragmentation which facilitates the unambiguous recognition of the elemental composition of the compounds, and the one- and two-dimensional ^{11}B NMR spectra help to provide initial information on the structures of the molecules.

The yields of carboranes formed during the pyrolyses obviously depends on the reaction temperature and molar ratio of the reactants. The recombination of n [BX] units and 2 [CX] fragments in Equation 7 describes the overall conversion, but not the course of molecular formation. Based on the idealized Equation 9, the yield of **2** was approximately 7 %, that of **1** approximately one third thereof.

A conceivable route (see Scheme 1) could be a) the reaction of [BX] with the carbene [CX_2] to give $X_2C{=}BX$; dimerization and halogen cleavage may give a cyclic carbon-carbon bridged tetraborane (XCBX)$_2$ intermediate which provides the first building block containing two carbon atoms. Such (RCBR')$_2$ molecules with both classical and non-classical structures have been synthesized many years ago.[4b,c] Subsequently in this process, intermediate (XCBX)$_2$ rearranges to bis(dihaloboryl)ethyne $X_2B{-}C{\equiv}C{-}BX_2$ which is enlarged by [BX] units leading to the stable perhalogenated carborane end products.

An alternative route b) could be the successive insertion of 2 [BX] units into tetrahaloethene to give trihalovinyl-dihaloborane $X_2C{=}CX(BX_2)$ and 1,2-dihalo-bis(dihaloboryl)ethene $(BX_2)XC{=}CX(BX_2)$ which by elimination of X_2 gives bis(dihaloboryl)ethyne $X_2B{-}C{\equiv}C{-}BX_2$ and finally adds more [BX] units to the stable perhalogenated carborane end products.

NMR spectra

The compound with the formula $C_2B_5Cl_7$ (**1**) shows one broad ^{13}C NMR signal at 107.5 ppm upon heteronuclear {^{11}B} decoupling and two ^{11}B NMR signals in a 3 : 2 ratio at 28 ppm and 52 ppm. In the ^{11}B^{11}B COSY NMR spectrum there is no cross-

Research Article
doi.org/10.1002/slct.202301653

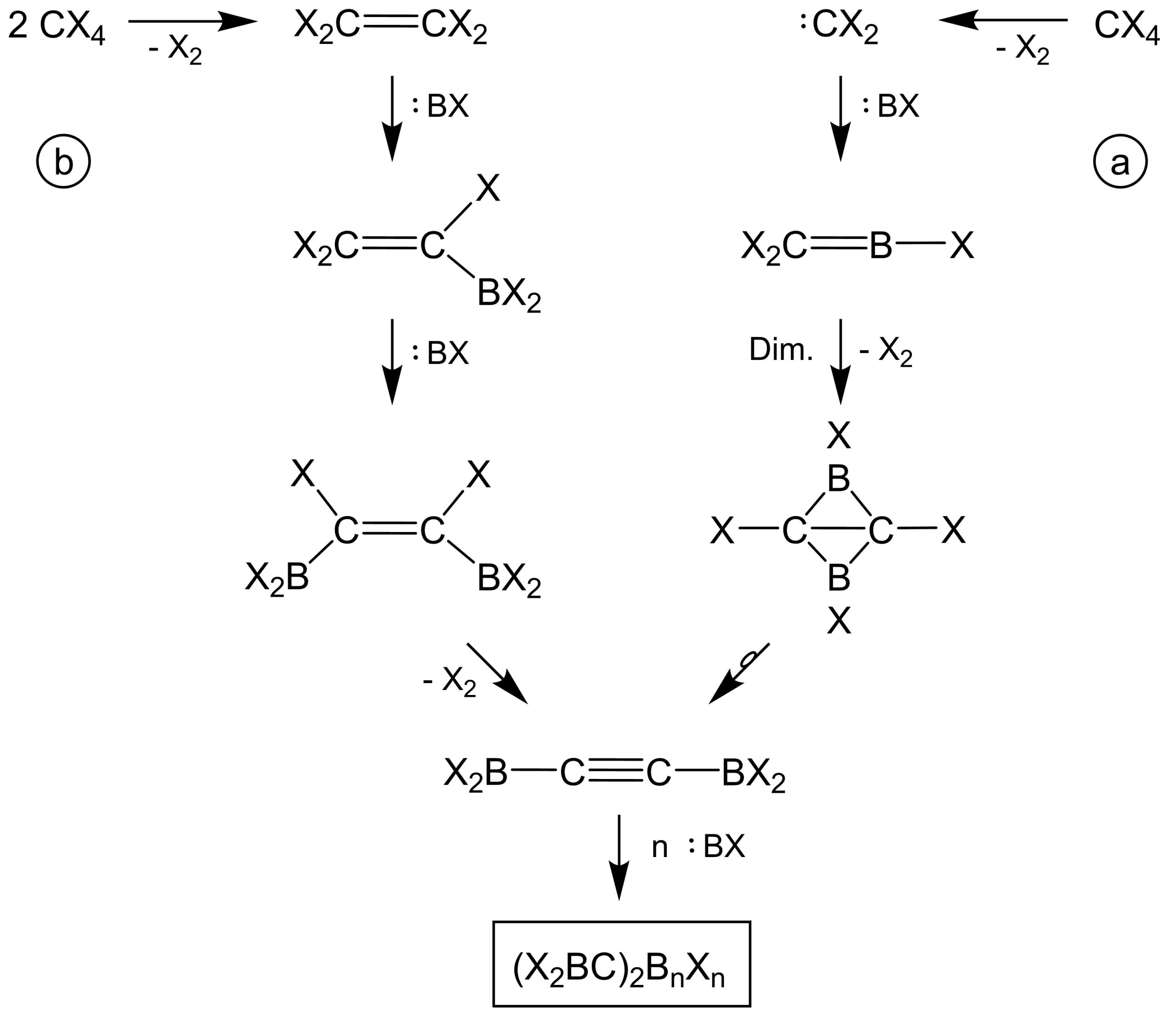

Scheme 1. Possible pathways for the formation of the perhalogenated carboranes **1** (X = Cl, n = 3), **2** (X = Cl, n = 5) and **3** (X = Br, n = 3).

peak-correlation detected (a technique which was not available at the time before our first short note in 1989, in addition to the poorer resolution of the available NMR spectrometers at that time). Therefore, our former assumption of a pentagonal-bipyramidal 2,4-$C_2B_5Cl_7$ carborane structure for **1** can be ruled out, since such a geometry should show two cross-peaks between three ^{11}B signals. ^{11}B NMR chemical shifts computed for alternative classical organoborane structures including a $C_2B_5Cl_7$ norbornane- and a dimeric $(C_2B_5Cl_7)_2$ adamantane-type geometry also do not fit the experimental values (see computational results). However, very good agreement was achieved for *closo*-1,5-$(CBCl_2)_2B_3Cl_3$ (**1**), a carborane structure with 2 *exo*-skeletal BCl_2 groups "classically" bonded at both C-atoms, as depicted in Figure 1: calculated values of 27.0 ppm (exp.: 28 ppm) for basal B(2–4) and 54.7 ppm (exp.: 52 ppm) for the *exo*-polyhedral BCl_2-groups. Analogous to **1**, the compound with the formula $C_2B_5Br_7$ (**3**) exhibits two ^{11}B NMR signals in a 3:2 ratio with calculated values of 20.3 ppm (exp.: 21.5 ppm) and 57.9 ppm (exp.: 53.3 ppm) in accordance with B(2-4) and the two *exo*-skeletal (BBr_2) groups of *closo*-1,5-$(CBBr_2)_2B_3Br_3$, respectively.

One of the few alternative routes to five-vertex *closo*-carboranes was reported 2002 by Siebert *et al.* with the synthesis and X-ray structure of 1,5-dineopentyl-2,3,4-trichloro-1,5-dicarba-*closo*-pentaborane(5) by pyrolysis of a bulky tris(dichloroboryl)alkane.[12] Both the ^{11}B ($\delta = 22.1$ ppm) and ^{13}C ($\delta = 94$ ppm) chemical shifts are in good agreement with the signals found for **1** and **3**.

The compound with the formula $C_2B_7Cl_9$ (**2**) shows one broad ^{13}C NMR signal at 91.0 ppm upon heteronuclear {^{11}B} decoupling and consists of four ^{11}B NMR signals with 2:2:1:2-intensities at −15.6 ppm, 8.8 ppm, 10.0 ppm and 54.8 ppm. In the ^{11}B^{11}B COSY NMR spectrum there are only two cross-peaks between the signal at the highest field and the signals at 8.8 and 10.0 ppm which is in contradiction to the formerly proposed "all-boron-*endo*" structure for **2** as *closo*-4,5-$C_2B_7Cl_9$. ^{11}B NMR chemical shifts computed for such a geometry as well as alternative classical organoborane structures including bicyclo[3.2.2] and bicyclo[3.3.1]-type geometries give no good agreement with the experimental values (see computational results) – again in contrast to a carborane isomer with 2 *exo*-skeletal BCl_2 groups of the formula "classically" bonded at both

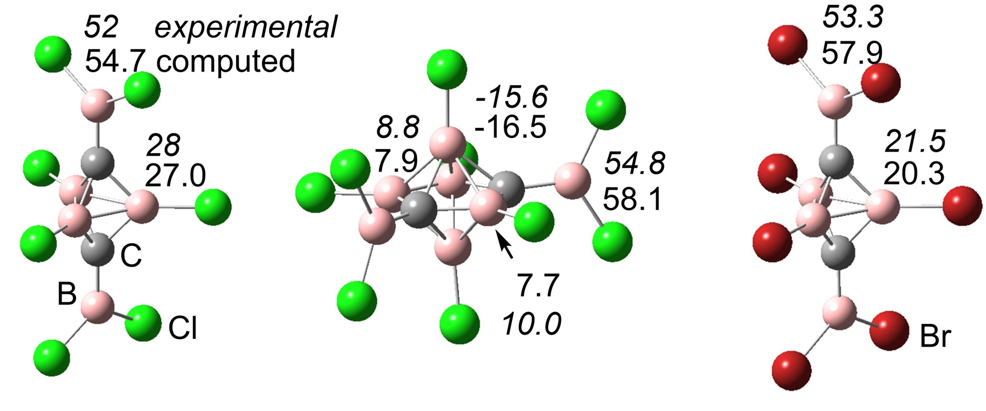

Figure 1. Experimental and computed ^{11}B NMR chemical shifts of $C_2B_5Cl_7$ (**1**), $C_2B_7Cl_9$ (**2**) and $C_2B_5Br_7$ (**3**).

C-atoms (see Figure 1). This suggests the most stable seven-vertex pentagonal-bipyramidal carborane geometry *closo*-2,4-$(CBCl_2)_2B_5Cl_5$ (**2**) with the ^{11}B NMR signal at −15.6 ppm (calcd.: −16.5 ppm) assigned to the apical B-atoms B(1,7), the signal at 8.8 ppm (calcd.: 7.9 ppm) to B(5,6), the intensity-one signal at 10 ppm (calcd.: 7.7 ppm) to B(3) and the signal at 54.8 ppm (calcd.: 58.1 ppm) to both *exo*-polyhedral BCl_2-groups. By cooling a sample of **2** in $CDCl_3$ to temperatures as low as −55 °C, the ^{11}B NMR signal of *exo*-skeletal BCl_2 at 54.8 ppm broadens in contrast to those of the cage B atoms which are not affected. The different temperature dependency of the ^{11}B NMR signals in **2** can be explained by dynamic phenomena of the more flexible *exo*-skeletal BCl_2 groups compared to the cage B-atoms and support the assignments in the above geometry.

In order to improve the resolution of ^{13}C NMR spectra and eventually to get more structural information about the positions of the C-atoms within the clusters, the carboranes **1** and **2** were subjected to detailed heteronuclear $^{13}C\{^{11}B\}$ decoupling experiments to simplify the complex spin systems. Once recorded ^{11}B undecoupled, the ^{13}C NMR signals of both **1** and **2** are hardly detectable. Upon selective boron decoupling of a sample of **2** in $CDCl_3$ the ^{13}C NMR signal resolves to a singlet at 90.27 ppm. Best resolution enhancement of the ^{13}C NMR signal could be obtained by ^{11}B broadband-decoupling at +20 ppm as well as at +54.8 ppm (see Figures S5 and S6). In a 1:1 mixture of the carboranes **1** and **2**, the ^{13}C signal of **1** at 107.5 ppm sharpens upon ^{11}B broadband-decoupling at +40 ppm which is midway between +52 ppm (*exo*-skeletal BCl_2 group) and +28 ppm (B2-4), whereas upon selective decoupling at +28 ppm or +52 ppm only the resolution is improved.

The ^{11}B NMR spectrum of $Br_2C{=}CBr{-}BBr_2$ (**4**) consists of one broad signal at 52.0 ppm ($h_{1/2} \approx 150$ Hz) which is in very good agreement with the calculated value of 55.0 ppm (see Figure S19 of Supporting Information). The mass spectral fragmentation of **4** is shown in Figure S12.

Mass spectra

The mass spectra of compounds **1**–**3** exhibit the isotopic patterns for the molecular ion and the main fragments indicating the stepwise abstraction of Cl, BCl_2, and mainly BCl_3 fragments whose intensity patterns are consistent with the computed spectra based on natural isotopic abundances.

Unfortunately, we could not obtain the carboranes in crystalline form, however, on the basis of simple skeletal electron counting rules,[8] **1**, **2** and **3** should adopt the geometries derived from the ^{11}B NMR spectra with each X_2B–C group contributing 3 electrons and each BX unit 2 electrons to the cluster bonding.

DFT/GIAO(ZORA)/NMR computations

Generally nonrelativistic computations were performed at the B3LYP/6-311+G(d,p)+ZPE DFT level.[13,14] For bromine substituted boron atoms, however, satisfactory agreement can only be expected when spin-orbit (SO) coupling is taken into account.[15a,b] This was done using the ZORA formalism[16] as implemented in the ADF program[17] (see Computational Details). Such SO-corrections were recently also found necessary even for such perchlorinated heteroboranes, in which heavy-chalcogen tellurium is part of the cluster.[15c]

Only cluster structures with dihaloboryl substituted carbon atoms give computed ^{11}B NMR chemical shifts that satisfactorily match the experimental values (see Figures S13, S14 and S15 of Supporting Information).

These "non-classical" polyhedral structures are unexpected for products from such pyrolysis reactions since it is empirically known in experimental carborane chemistry, that high-energy reaction conditions during synthesis favor the formation of "all-*endo*" *closo*-carboranes such as **C** in Figures 2 and 3 with the most stable positional isomers having the carbon atoms in positions 2,4 for pentagonal-bipyramidal $C_2B_5X_7$ and 4,5 for tricapped trigonal-prismatic $C_2B_7X_9$, while low-energy conditions favor alkylboranes and *nido*-carboranes. Nevertheless,

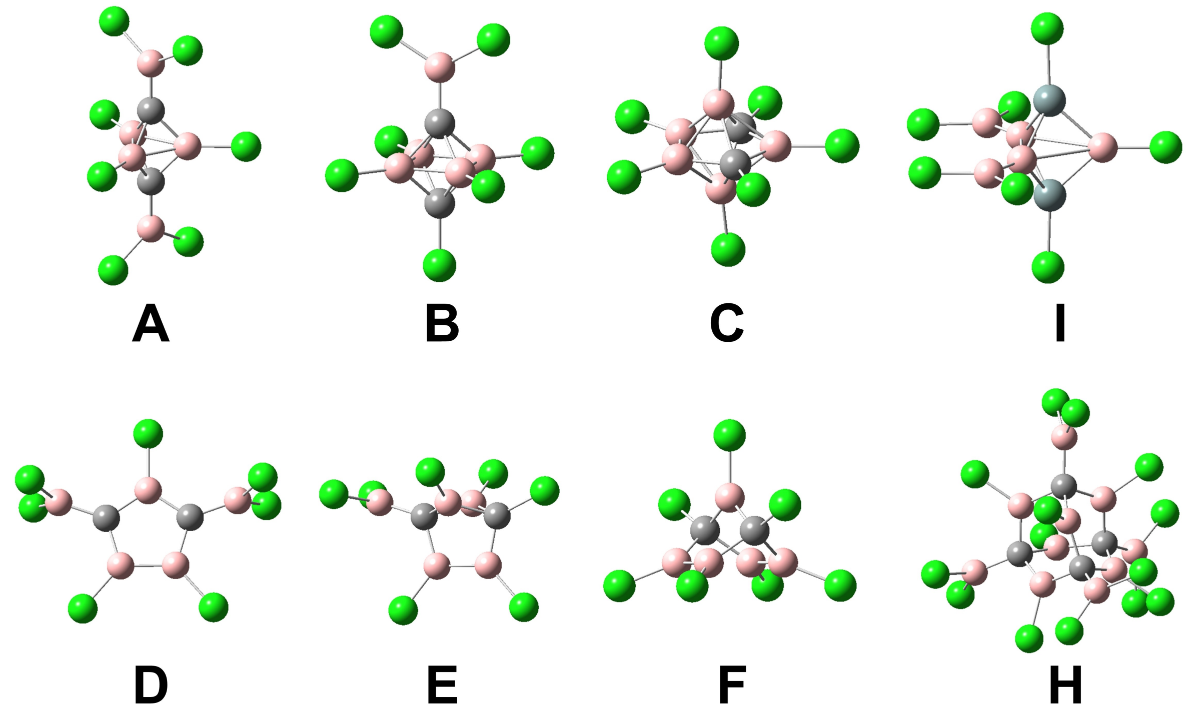

Figure 2. Various $C_2B_5X_7$ isomers **A**–**F**, **I** as well as the dimeric $C_4B_{10}X_{14}$ with adamantane structure, **H** (X = H, Cl, Br). C, B and X are shown in grey, pink and green, respectively.

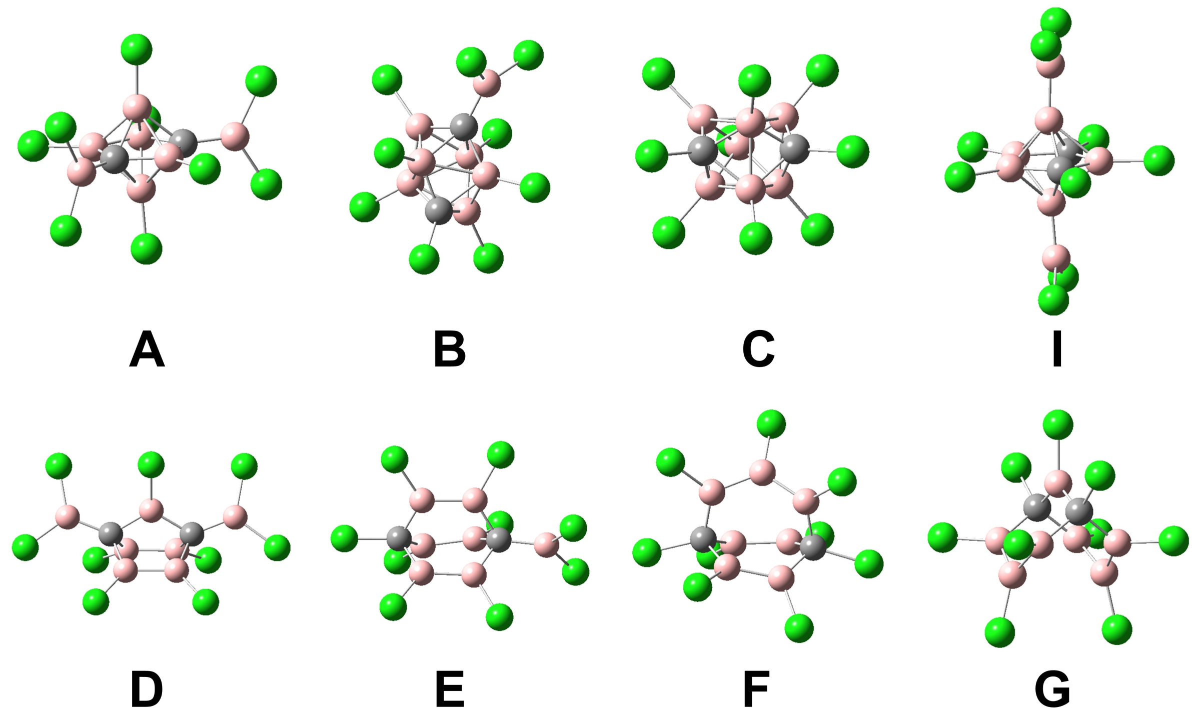

Figure 3. Various $C_2B_7X_9$ isomers **A**–**I** (X = H, Cl, Br). C, B and X are shown in grey, pink and green, respectively.

computations show that they are thermodynamically more stable than the expected cluster structures (type **C**) and classical cyclic or bicyclic structures such as types **D**, **E** and **F** when they are perhalogenated. For the parent carboranes with H substituents the expected *closo*-cluster with all boron atoms of the formula *endo*-skeletally incorporated into the cluster framework is thermodynamically favored. Relative energy values are listed in Table 1 and Table 2 for $C_2B_5X_7$ and $C_2B_7X_9$

Table 1. Relative energies in kcal mol^{-1} computed for $E_2B_5X_7$ isomers at B3LYP/6-311+G(d,p)+ZPE.

E	*X*	A	B	C	D	E	F	H [a]	I
C	H	0.0	−11.6	−38.9	58.5 [b]	8.0	20.0	−3.4	14.9
	Cl	0.0	49.9	69.9	46.2 [b]	40.4	80.8	−6.8	80.0
	Br	0.0	41.8	57.1	42.9 [b]	35.8	71.4	2.0	69.1
Si	H	0.0	−47.9	−67.5	10.5 [b]	−11.2 [c]	20.0	−4.5	−8.0
	Cl	0,0	−24.1	−38.0	−10.0 [b]	−6.2	−9.1	−29.9	−10.1

[a] Type **H** corresponds to $E_4B_{10}X_{14}$ with an adamantane structure. The energy values given refer to one half of this molecule relative to one **A**. [b] Two imaginary frequencies in C_{2v}. Optimizations in lower symmetry point groups lead to different structures. [c] Optimized geometry is strongly distorted.

Table 2. Relative energies in kcal mol^{-1} computed for $E_2B_7X_9$ isomers at B3LYP/6-311+G(d,p)+ZPE.

E	*X*	A	B	C	D	E	F	G	I
C	H	0.0	−7.2	−27.7	59.1	–[a]	–[a]	70.5[b]	22.0
	Cl	0.0	38.6	68.7	25.7	63.2	108.1	112.3	76.2
	Br	0.0	33.9	57.7	30.9	61.2	98.7	104.7	66.4
Si	H	0.0[c]	−37.8	−37.0	90.2[d]	–[a]	–[a]	47.1	−0.3
	Cl	0.0[e]	−24.6	−10.0	31.7	27.4	28.6	26.1	−11.6

[a] Rearranged upon optimization. [b] Two imaginary frequencies in C_{2v}. Optimizations in lower symmetry point groups lead to different structures. [c] The 1,7-$(H_2BSi)_2B_5H_5$ isomer is more stable by 19.7 kcal mol^{-1} than the 2,4-isomer. For direct comparison with the carbon analogs the 2,4-isomer was nevertheless chosen as the reference point. [d] Two imaginary frequencies in C_s. Without symmetry constrains geometry optimization lead to the *closo*-2,4-$(H_2BSi)_2B_5H_5$ structure. [e] The 1,7-$(Cl_2BSi)_2B_5Cl_5$ isomer is more stable by 21.6 kcal mol^{-1} than the 2,4-isomer. For direct comparison with the carbon analogs the 2,4-isomer was nevertheless chosen as the reference point.

isomers (X=H, Cl, Br), respectively. Only the dimeric adamantane framework **H** is slightly more stable (by 6.8 kcal for one mol of $C_2B_5Cl_7$).

The medium sized cluster with only one boryl substituted carbon atom (type **B**) is also more stable than the expected type **C**, but a second dihalogenboryl carbon moiety brings a larger stability gain than the first one (i.e. **A** vs. **B** in comparison to **B** vs. **C**). Boryl groups are only energetically advantageous when they are bound to carbon atoms: Structure type **I** with two boryl groups as boron rather than carbon substituents as in **A** has always a higher energy even than the Wade type cluster **C** without boryl groups. We also computed corresponding disilaboranes and found that among both the hydrogen as well as the chlorine compounds Wade type *closo*-clusters are thermodynamically more stable than isomers with boryl groups attached to the silicon atoms.

The stability order of different carbon atom placements in the cluster is unchanged by the presence of boryl substituents. Although relative energy values differ somewhat, they increase in the order 1,5-<1,2-<2,3- for the five vertex clusters (see Figure S17) and 2,4-<2,3-<1,2-<1,7- for the seven vertex clusters (see Figure S18) for both dichloroboryl and chlorine substituted carbon atoms.

Conclusions

The herein presented pyrolytic route to trigonal- and pentagonal-bipyramidal carboranes **1**, **2** and **3** from simple, electron-precise synthons diboron tetrahalides and halocarbons provides a new, rare alternative access to the smallest carborane motif. The experimentally observed and computationally confirmed *exo-endo* isomerism of perhalogenated carboranes to assemble in unusual structures with *exo*-skeletal $BHal_2$ groups attached to both carbon atoms is unprecedented within the family of the *closo*-dicarboranes $C_2B_nX_{n+2}$. The thermodynamic stabilization of **1**, **2**, and **3** stands in sharp contrast to the classical (*endo*) Wade type parent compounds with X=H as well as with the corresponding isoelectronic *closo*-disilaboranes either with hydrogen or with chlorine ligands. Only the limited yields of **1**, **2** and **3** in low mg-scales prevented us so far from exploring their reactivities, in particular attempts of full hydrogenations to the parent compounds with expected rearrangements to classical Wade type *closo*-dicarboranes.

Experimental Section

Instrumentation. ^{11}B NMR spectra were partly recorded on Bruker instruments WM-250 (^{11}B 80.25 MHz), AVANCE III 500 (^{11}B 160.388 MHz) and AVANCE III HD 600 (^{11}B 192.552 MHz) at 293 K if not stated otherwise. $^{13}C\{^{11}B\}$ NMR spectra were recorded on a Bruker AVANCE III HD 300 spectrometer (^{13}C 75.48 MHz). Chemical shifts were referenced to external $BF_3 \cdot OEt_2$ and TMS. Negative signs indicate an upfield shift. The NMR spectra were processed using SpinWorks 4 (v 4.2.3.0 Kirk Marat, University of Manitoba, Canada) software. High- and low-resolution mass spectra were obtained on a Finnigan Varian MAT 95 with electron ionization at 70 eV.

General Procedures and Materials. All manipulations were conducted in a standard high vacuum-line or by using inert atmosphere techniques with glassware equipped with PTFE valves (J. Young Scientific Glassware, Acton, London) and O-ring seals for greaseless connection to the vacuum-line as described by Shriver.[18] Inert gas N_2 and solvents were reagent grade, dried and purified according to standard procedures. BCl_3 was purified by vacuum fractionation until a vapor pressure of 4 Torr at −78 °C was obtained. BBr_3 was stirred over mercury, degassed, and condensed into a trap of −78 °C prior to use. The diboron tetrahalides B_2Cl_4 and B_2Br_4 were prepared by co-condensation of BCl_3 or BBr_3 with copper-vapor onto cooled walls (−196 °C) of a metal-vapor reactor similar to that described by Timms.[19] After reaction, B_2Hal_4 was separated from excess $BHal_3$ by repeated fractionation until the condensate exhibited a vapor pressure at 0 °C of 44 Torr (B_2Cl_4) or less than 1 Torr (B_2Br_4).

Syntheses of $C_2B_5Cl_7$ (1) and $C_2B_7Cl_9$ (2). In a typical pyrolysis, samples of B_2Cl_4 (3.3 g, 20.2 mmol) and C_2Cl_4 (5.7 g, 34.4 mmol) were separately condensed *in vacuo* into a 250-mL round-bottomed flask equipped with a seal-constriction and a break-seal joint. After sealing, the flask was heated in an oven at 350 °C for 30 minutes, and slowly allowed to cool to room temperature over a period of 20 h resulting in black precipitation (possibly graphite or boroncarbide). After connecting to the vacuum-line, the break-seal was opened under vacuum and ca. 15 mL BCl_3 was condensed into the flask to extract the products repeatedly 10 times into a separate flask. The part which was insoluble in BCl_3 was separated *in vacuo* by a frit and washed out 5 times with the 15 mL BCl_3. After evaporation of the extractant BCl_3 at temperatures below −30 °C, the residue was dissolved in ca. 1 mL CH_2Cl_2 and ^{11}B NMR spectrum indicated a proportion of the main products $C_2B_5Cl_7$: $C_2B_7Cl_9$: B_9Cl_9 of 1.25:3.75:1. After evaporation of CH_2Cl_2 at −10 °C the residue separated *in vacuo* (10^{-3} mbar) into 4 fractions which were analyzed by ^{11}B NMR and MS: a) volatiles between −10 °C and 10 °C: contains only carboranes, mainly **1** and less **2**, no B_9Cl_9; b) volatiles between 10 °C and 40 °C: mainly **2**, less **1** and B_9Cl_9. c) volatiles between 40 °C and 90 °C: mainly **2** and B_9Cl_9, no **1**; d) volatiles between 90 °C and strong heating with the heat-gun (ca. 300 °C): mainly B_9Cl_9, $B_{10}Cl_{10}$, very little **2**. It was not possible to separate **1** and **2** from fraction a). A pure sample of **2** was obtained by performing co-pyrolysis at 450 °C and trapping all volatiles between 0 °C and 300 °C which contained only **2** and C_6Cl_6, no B_9Cl_9 as well as **1**. C_6Cl_6 could be separated by vacuum-sublimation at T ≈ 40 °C. The yield of purified **2** was averaged 75 mg (7 % based on idealized Equation 9) per co-pyrolysis. The yield of **1**, which only could be enriched, was based on the ^{11}B NMR spectra only a third thereof.

Syntheses of $C_2B_5Br_7$ (3) and $Br_2C{=}CBr\text{-}BBr_2$ (4).[20] Samples of B_2Br_4 (1.5 g, 4.4 mmol) and CBr_4 (0.5 g, 1.5 mmol) were separately condensed *in vacuo* into a 250-mL round-bottomed flask equipped with a seal-constriction and a break-seal joint. After sealing, the flask was heated in an oven at 300 °C for 30 min, and slowly allowed to cool to room temperature over a period of 20 h resulting in black-shining solid (possibly graphite or boroncarbide). After connecting to the vacuum-line, the break-seal was opened under vacuum and ca. 15 mL BBr_3 was condensed into the flask to extract the products repeatedly 10 times into a separate flask. The part which was insoluble in BBr_3 was separated from the soluble part *in vacuo* by a frit and the residue washed out 5 times again with the 15 mL BBr_3. After evaporation of the extractant BBr_3 from the soluble part at temperatures below 0 °C, the residue was fractionated *in vacuo* to yield at $T_{subl.}$ ≈ 200 °C 10 mg of **3** as a white solid. Other products, detected by MS and ^{11}B NMR, were tetrabromoethene C_2Br_4 in the more volatile fraction between room temperature and 100 °C/HV, and the boronsubbromides B_nBr_n (n = 7–10) in the less volatile fractions between 100 °C and 200 °C. Traces in the MS with a pattern at m/e = 728 indicate the generation of very small amounts of the next higher member $C_2B_6Br_8$.

For preparation of $Br_2C{=}CBr\text{-}BBr_2$ (**4**) the co-pyrolysis of B_2Br_4 with C_2Br_4 was performed at 220 °C. Work-up as described above yielded **4** as colorless liquid with a bp ≈ 100 °C/HV.

Data for **1**: MS *m/z* (rel. int.): 326 (93, M^+); 291 (100, $[M–Cl]^+$); 210 (95, $[M\text{-}BCl_3]^+$); exact mass calcd for $^{12}C_2{}^{11}B_5{}^{35}Cl_7$ 324.8292; found 324.8285; ^{11}B NMR (ppm, $CDCl_3$) 28.0 (B2-4), 52.0 (*exo*-BCl_2), no cross-peak in ^{11}B^{11}B COSY NMR; ^{13}C{^{11}B} NMR (ppm, $CDCl_3$) 107.5 (C1,5).

Data for **2**: MS *m/z* (rel. int.): 418 (75, M^+); 383 (3, $[M–Cl]^+$); 337 (20, $[M\text{-}BCl_2]^+$); 302 (100, $[M\text{-}BCl_3]^+$); 291 (33, $[M\text{-}B_2Cl_3]^+$); 219 (35, $[M\text{-}B_2Cl_5]^+$); 185 (55, $[M\text{-}2BCl_3]^+$); 150 (30, $[B_4Cl_3]^+$); 114 (36, $[B_4Cl_2]^+$); 103 (33, $[B_3Cl_2]^+$); 81 (170, $[BCl_2]^+$); exact mass calcd for $^{12}C_2{}^{11}B_7{}^{35}Cl_9$ 418.7829; found 418.7825; ^{11}B NMR (ppm, $CDCl_3$) −15.6 (B1,7), 8.8 (B5,6), 10.0 (B3), 54.8 (*exo*-BCl_2) with cross-peaks of B(1,7) with B(5,6) and B(3) in ^{11}B^{11}B COSY NMR; ^{13}C{^{11}B} NMR (ppm, $CDCl_3$) 91.0 ppm (C2,4).

Data for **3**: MS *m/z* (rel. int.): 637 (58, M^+); 558 (100, $[M–Br]^+$); 365 (30, $[M–CB_2Br_3]^+$); 307 (30, $[M\text{-}BBr_4]^+$); 228 (10, $[C_2B_4Br_2]^+$); 205 (15, $[CB_3Br_2]^+$); 194 (10, $[CB_2Br_2]^+$); 171 (90, $[BBr_2]^+$);^{11}B NMR (ppm, $CDCl_3$) 21.5 (B2-4), 53.3 (*exo*-BBr_2).

Data for $Br_2C{=}CBr\text{-}BBr_2$ (**4**): MS *m/z* (rel. int.): 434 (58, M^+); 355 (100, $[M–Br]^+$); 275 (13, $[M\text{-}2Br]^+$); 195 (45, $[M\text{-}3Br]^+$); 171 (82, $[BBr_2]^+$); 91 (10, $[BBr]^+$); ^{11}B NMR: 52.0 ppm ($h_{1/2}$ ≈ 150 Hz).

Computational Details. Geometries were optimized using the Gaussian 16 program[21] employing the B3LYP hybrid density functional[13] and the 6–311 + G(d,p) basis set.[14] Subsequent frequency calculations revealed the nature of the stationary points and gave zero point vibrational energies (ZPE). Relative energies reported correspond to the B3LYP/6-311 + G(d,p) + ZPE level. Magnetic shielding constants were computed at the same level using the GIAO approach.[22] For brominated molecules the ADF engine[17] of the Amsterdam Modeling Suite[23] was used to compute shielding constants employing GIAOs and the B3LYP hybrid functional together with the TZP (polarized triple zeta) basis[24] including spin orbit coupling using the zeroth-order regular approximation (ZORA)[16] for relativistic effects.[25] While computed ^{13}C chemical shifts are directly referenced to tetra methyl silane, ^{11}B chemical shifts were initially calculated relative to diborane(6) and converted to the experimental standard, $BF_3{\cdot}O(C_2H_5)_2$, using the chemical shift value of 16.6 ppm reported for B_2H_6.[26]

Supporting Information Summary

The Supporting Information contains experimental ^{11}B, ^{11}B^{11}B COSY, ^{13}C{^{11}B} NMR, MS and HR-MS spectra, in addition, calculated ^{11}B and ^{13}C NMR chemical shifts, computed with GIAO(ZORA) at B3LYP/6-311 + G(d,p), absolute and relative energies as well as optimized Cartesian coordinates of all relevant compounds included in this work.

Acknowledgements

Support of this work by the Deutsche Forschungsgemeinschaft (DFG Schwerpunktprogramm Polyeder) is gratefully acknowledged. The authors acknowledge support by the state of Baden-Württemberg through bwHPC and the German Research Foundation (DFG) through grant no INST 40/575-1 FUGG (JUSTUS 2 cluster). We also thank Mr. Mario Wolf (Institut für Chemie, *Universität Hohenheim) for recording the ^{11}B NMR spectra, Dipl.-Ing. (FH) Joachim Trinkner (Institut für Organische Chemie, Universität Stuttgart) for performing the mass spectrometry, Prof. Dr. Dr. h.c. Wolfgang Haubold for financial support, and Dr. Rüdiger Bertermann and Prof. Dr. Maik Finze (Institut für Anorganische Chemie, Julius-Maximilians-Universität Würzburg) for recording and discussing the ^{13}C{^{11}B} spectra. Open Access funding enabled and organized by Projekt DEAL.*

Conflict of Interests

The authors declare no conflict of interest.

Data Availability Statement

The data that supports the findings of this study are available in the supplementary material of this article.

Keywords: *closo*-dicarbaboranes · *closo*-disilaboranes · DFT/GIAO(ZORA)/NMR · *exo-endo* Isomerism · perhalogenated Boranes

[1] I. Shapiro, C. D. Good, R. E. Williams, *J. Am. Chem. Soc.* **1962**, *84*, 3837–3840.
[2] a) P. v. R. Schleyer, G. Subramanian, A. Dransfeld, *J. Am. Chem. Soc.* **1996**, *118*, 9988–9989; b) R. N. Camp, D. S. Marynick, G. D. Graham, W. N. Lipscomb, *J. Am. Chem. Soc.* **1978**, *100*, 6781–6783; c) M. L. McKee, *J. Am. Chem. Soc.* **1988**, *110*, 5317–5321.
[3] a) K. Krogh-Jespersen, D. Cremer, J. D. Dill, J. A. Pople, P. v. R. Schleyer, *J. Am. Chem. Soc.* **1981**, *103*, 2589–2594; b) P. M. Budzelaar, K. Krogh-Jespersen, T. Clark, P. v. R. Schleyer, *J. Am. Chem. Soc.* **1985**, *107*, 2773–2779; c) M. Hofmann, M. A. Fox, R. Greatrex, P. v. R. Schleyer, J. W. Bausch, R. E. Williams, *Inorg. Chem.* **1996**, *35*, 6170–6178; d) F. A. McNeill, K. L. Gallaher, F. R. Scholer, S. H. Bauer, *Inorg. Chem.* **1973**, *12*, 2108-2111; e) M. Antipin, R. Boese, D. Bläser, A. Maulitz, *J. Am. Chem. Soc.* **1997**, *119*, 326-333.
[4] a) M. L. McKee, *Inorg. Chem.* **2000**, *39*, 4206–4210; b) M. Hildenbrand, H. Pritzkow, U. Zenneck, W. Siebert, *Angew. Chem. Int. Ed.* **1984**, *23*, 371–372; c) M. Unverzagt, G. Subramanian, M. Hofmann, P. v. R. Schleyer, S. Berger, K. Harms, W. Massa, A. Berndt, *Angew. Chem. Int. Ed.* **1997**, *36*, 1469–1472.
[5] W. Haubold, W. Keller, G. Sawitzki, *J. Organomet. Chem.* **1989**, *367*, 19–25.
[6] W. Haubold, W. Keller, *J. Organomet. Chem.* **1989**, *361*, 54–56.
[7] W. Haubold, W. Keller, G. Sawitzki, *Angew. Chem. Int. Ed.* **1988**, *27*, 925–926.
[8] a) R. E. Williams, *Inorg. Chem.* **1971**, *10*, 210–214; b) K. Wade, *Adv. Inorg. Chem. Radiochem.* **1976**, *18*, 1–66; c) R. E. Williams, *Adv. Inorg. Chem. Radiochem.* **1976**, *18*, 67–142; d) R. W. Rudolph, *Acc. Chem. Res.* **1976**, *9*, 446–452; e) R. E. Williams, *Electron Deficient Boron and Carbon Clusters* (Eds.: G. A. Olah, K. Wade, R. E. Williams), Wiley and Sons, New York, **1991**, 11–93.
[9] Review: J. A. Morrison, *Advances in Boron and the Boranes* (Eds.: J. F. Liebman, A. Greenberg, R. E. Williams), VCH Publishers, New York, **1988**, 151–189.
[10] B. Solouki, H. Bock, R. Weinmann, W. Haubold, unpublished results; citation in R. Weinmann, *Dissertation*, Universität Stuttgart, **1985**.
[11] a) R. Steudel, *Zeitschrift für Naturforschung B* **1968**, *23*, 1163–1171; b) T. Tsuge, J. J. Leary, T. L. Isenhour, *J. Chem. Educ.* **1974**, *51*, 266–267.
[12] M. J. Bayer, H. Pritzkow, W. Siebert, *Eur. J. Inorg. Chem.* **2002**, 1293–1300.
[13] a) A. D. Becke, *J. Chem. Phys.* **1993**, *98*, 5648–5652; b) C. Lee, W. Yang, R. G. Parr, *Phys. Rev. B* **1988**, *37*, 785–789; c) S. H. Vosko, L. Wilk, M. Nusair, *Can. J. Phys.* **1980**, *58*, 1200–1211; d) P. J. Stephens, F. J. Devlin, C. F. Chabalowski, M. J. Frisch, *J. Phys. Chem.* **1994**, *98*, 11623–11627.
[14] a) A. D. McLean, G. S. Chandler, *J. Chem. Phys.* **1980**, *72*, 5639–5648; b) K. Raghavachari, J. S. Binkley, R. Seeger, J. A. Pople, *J. Chem. Phys.* **1980**, *72*, 650–654; c) M. J. Frisch, J. A. Pople, J. S. Binkley, *J. Chem. Phys.* **1984**, *80*, 3265–3269; d) T. Clark, J. Chandrasekhar, G. W. Spitznagel, P. v. R. Schleyer, *J. Comput. Chem.* **1983**, *4*, 294–301.
[15] a) M. Kaupp, *Theoretical and Computational Chemistry* (Ed.: P. Schwerdtfeger), Elsevier, Amsterdam, **2004**, Vol. 14, 552–597; b) W. Keller, M. Hofmann, M.-B. Sárosi, J. Fanfrlík, D. Hnyk, *Inorg. Chem.* **2022**, *61*, 16565–16572; c) W. Keller, J. Ballmann, M. B. Sárosi, J. Fanfrlík, D. Hnyk, *Angew. Chem. Int. Ed.* **2023**, doi.org/anie.202219018.
[16] a) E. van Lenthe, E. J. Baerends, J. G. Snijders, *J. Chem. Phys.* **1993**, *99*, 4597–4610; b) E. van Lenthe, E. J. Baerends, J. G. Snijders, *J. Chem. Phys.* **1994**, *101*, 9783–9792; c) E. van Lenthe, J. G. Snijders, E. J. Baerends, *J. Chem. Phys.* **1996**, *105*, 6505–6516.
[17] a) G. te Velde, F. M. Bickelhaupt, E. J. Baerends, C. Fonseca Guerra, S. J. A. van Gisbergen, J. G. Snijders, T. Ziegler, *J. Comput. Chem.* **2001**, *22*, 931–967; b) E. J. Baerends, J. Autschbach, A. Bérces, C. Bo, P. M. Boerrigter, L. Cavallo, D. P. Chong, L. Deng, R. M. Dickson, D. E. Ellis, L. Fan, T. H. Fischer, C. Fonseca Guerra, S. J. A. van Gisbergen, J. A. Groeneveld, O. V. Gritsenko, M. Grüning, F. E. Harris, P. van den Hoek, H. Jacobsen, G. van Kessel, F. Kootstra, E. van Lenthe, D. A. McCormack, V. P. Osinga, S. Patchkovskii, P. H. T. Philipsen, D. Post, C. C. Pye, W. Ravenek, P. Ros, P. R. T. Schipper, G. Schreckenbach, J. G. Snijders, M. Sola, M. Swart, D. Swerhone, G. te Velde, P. Vernooijs, L. Versluis, O. Visser, E. van Wezenbeek, G. Wiesenekker, S. K. Wolff, T. K. Woo, T. Ziegler, ADF2004.01, SCM, Theoretical Chemistry, Vrije Universiteit, Amsterdam, Netherlands, **2004**.
[18] D. F. Shriver, M. A. Drezdon, *The Manipulation of Air-Sensitive Compounds*, 2nd ed., John Wiley & Sons, New York, **1986**.
[19] P. L. Timms, *Adv. Inorg. Chem. Radiochem.* **1972**, *14*, 121–171.
[20] W. Keller, *Dissertation*, Universität Stuttgart, **1987**.
[21] Gaussian 16, Revision C.01, M. J. Frisch, G. W. Trucks, H. B. Schlegel, G. E. Scuseria, M. A. Robb, J. R. Cheeseman, G. Scalmani, V. Barone, G. A. Petersson, H. Nakatsuji, X. Li, M. Caricato, A. V. Marenich, J. Bloino, B. G. Janesko, R. Gomperts, B. Mennucci, H. P. Hratchian, J. V. Ortiz, A. F. Izmaylov, J. L. Sonnenberg, D. Williams-Young, F. Ding, F. Lipparini, F. Egidi, J. Goings, B. Peng, A. Petrone, T. Henderson, D. Ranasinghe, V. G. Zakrzewski, J. Gao, N. Rega, G. Zheng, W. Liang, M. Hada, M. Ehara, K. Toyota, R. Fukuda, J. Hasegawa, M. Ishida, T. Nakajima, Y. Honda, O. Kitao, H. Nakai, T. Vreven, K. Throssell, J. A. Montgomery Jr., J. E. Peralta, F. Ogliaro, M. J. Bearpark, J. J. Heyd, E. N. Brothers, K. N. Kudin, V. N. Staroverov, T. A. Keith, R. Kobayashi, J. Normand, K. Raghavachari, A. P. Rendell, J. C. Burant, S. S. Iyengar, J. Tomasi, M. Cossi, J. M. Millam, M. Klene, C. Adamo, R. Cammi, J. W. Ochterski, R. L. Martin, K. Morokuma, O. Farkas, J. B. Foresman, D. J. Fox, Gaussian, Inc., Wallingford CT, **2016**.
[22] K. Ruud, T. Helgaker, K. L. Bak, P. Jørgensen, H. J. A. Jensen, *J. Chem. Phys.* **1993**, *99*, 3847–3859.
[23] R. Rüger, M. Franchini, T. Trnka, A. Yakovlev, E. van Lenthe, P. Philipsen, T. van Vuren, B. Klumpers, T. Soini. AMS 2022.102, SCM, Theoretical Chemistry, Vrije Universiteit, Amsterdam, The Netherlands, http://www.scm.com.
[24] E. van Lenthe, E. J. Baerends, *J. Comput. Chem.* **2003**, *24*, 1142–1156.
[25] a) G. Schreckenbach, T. Ziegler, *J. Phys. Chem.* **1995**, *99*, 606–611; b) M. Krykunov, T. Ziegler, E. van Lenthe, *Int. J. Quantum Chem.* **2009**, *109*, 1676–1683; c) S. K. Wolff, T. Ziegler, *J. Chem. Phys.* **1998**, *109*, 895–905; d) S. K. Wolff, T. Ziegler, E. van Lenthe, E. J. Baerends, *J. Chem. Phys.* **1999**, *110*, 7689–7698.
[26] T. P. Onak, H. L. Landesman, R. E. Williams, I. Shapiro, *J. Phys. Chem.* **1959**, *63*, 1533–1535.

Submitted: April 26, 2023
Accepted: May 31, 2023